Temporally and spatially resolved optical experiments on semiconductor quantum wells and quantum dots

G. von Plessen and J. Feldmann
Sektion Physik, Ludwig-Maximilians-Universitat,
D-80799 München, Germany

Received February 2, 1997

We study the relaxation dynamics of electron-hole pairs in semiconductor quantum wells and quantum dots. Temporally and spatially resolved optical pump-and-probe experiments are performed on strained (GaIn)As/Ga(PAs) quantum wells to gain information on the relaxation dynamics of excitons with *non-zero* in-plane center-of-mass momentum. The results of these measurements clearly show the cooling and heating dynamics of exciton distributions spread in momentum space. To study carrier relaxation in a zero-dimensional system, time-resolved photoluminescence experiments are performed on strain-induced (GaIn)As/GaAs quantum dots. A sub-picosecond onset of the quantum-dot photoluminescence at high excitation densities is observed, which shows that carrier relaxation into energetically low-lying quantum-dot states can be extremely fast. The rise time of this onset shows a density dependence that is consistent with carrier relaxation via Coulomb scattering. From the decay of the transients, the time constant for acoustic-phonon-induced scattering of electrons between quantum-dot levels is extracted.

I. Introduction

Ultrafast laser spectroscopy has been used extensively to study carrier relaxation phenomena in semiconductors and semiconductor nanostructures. This has lead to a good understanding of many aspects of carrier thermalization and recombination after optical excitation, in particular in III-V quantum well (QW) structures [1]. However, there is a basic problem when using light-matter interaction to study carrier relaxation in crystals. As a consequence of (i) the conservation law for the total momentum and (ii) the vanishing momentum of visible light as compared to the extension of the Brillouin zone, *only electron-hole (e-h) pair transitions with vanishing total wavevector* ($\vec{K} \approx 0$) *can be excited and detected,* provided no other quasi-particle that carries momentum is involved in the optical transition. In this sense, it is difficult to gain information on the relaxation dynamics of the *entire* e-h pair distribution in translationally invariant systems using optical experiments.

In the present article, we wish to illuminate this problem from two sides. First, we will show that it is possible to study the dynamics of e-h pairs with non-zero in-plane wavevector ($\vec{K}_{\|} \neq 0$) in QW's by making use of the fact that the momentum distribution of those e-h pairs is reflected in their spatial motion. To this end, we perform temporally and spatially resolved optical pump- probe experiments on strained (GaIn)As/Ga(PAs) QW's. We study the lateral diffusivity of excitons as a function of time and crystal temperature. These measurements allow the investigation of the cooling and heating dynamics of exciton distributions spread in $\vec{K}_{\|}$-space (Section II of this article). Second, we study carrier relaxation in quantum dots (QDs) that are produced by introducing a lateral confinement potential in the plane of a (GaIn)As/GaAs QW. The lateral carrier localization results in relaxing the $\vec{K}_{\|}$-selection rule in the coupling to the light field. This allows to optically monitor the relaxation dynamics of the entire e-h distribution in the QD, without the

$\vec{K}_{\|}$-conservation problems described above. We perform time-resolved photoluminescence experiments on the QD structure, and obtain information on the roles of Coulomb and phonon scattering and of phase-space filling in the carrier relaxation in the QD's (Section III of this article).

II. Relaxation dynamics in quantum wells

In this Section of the paper, we will show that it is possible to study the dynamics of QW e-h pairs with non-zero in-plane wavevector $\vec{K}_{\|} \neq 0$) by making use of the fact that the momentum distribution of those e-h pairs is reflected in their spatial motion. To illustrate the situation, let us consider Fig. 1, which schematically shows the dispersion relation of QW excitons in $\vec{K}_{\|}$ space. Let us assume that e-h pairs are excited at the continuum edge, near $\vec{K}_{\|} = 0$. Via interaction with acoustic phonons or static disorder potentials, they can subsequently scatter to the 1s branch of the exciton dispersion, hereby forming excitons. Since this process releases the excitonic binding energy to the excitons in the form of kinetic energy, a non-equilibrium exciton distribution with some excess energy with respect to the minimum of the 1s exciton dispersion is created. This distribution will rapidly thermalize and can then be characterized by an exciton temperature, T_X. This hot exciton distribution will subsequently equilibrate with the lattice, e.g. cool down to the lattice temperature T_L if initially $T_X > T_L$. The experimental technique which we use here relies on analyzing the lateral motion of excitons in the QW plane. In QW's, the kinetic energy and thus the lateral velocity of excitons are directly related to $\vec{K}_{\|}$. Accordingly, the lateral diffusion constant depends critically on the exciton distribution in $\vec{K}_{\|}$ space, which changes e.g. with exciton temperature. Therefore the measurement of the temporal evolution of the excitonic diffusivity is expected to reveal the relaxation dynamics of the ensemble of excitons spread in $\vec{K}_{\|}$ space. To monitor the lateral motion of the excitons, we perform temporally and spatially resolved optical pump-probe experiments on strained (GaIn)As/Ga(PAs) quantum wells, as described in the following.

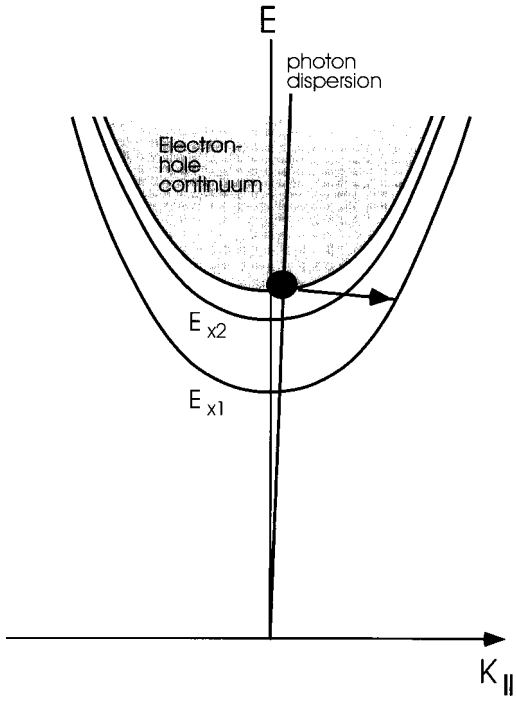

Figure 1. Schematic dispersion relation of excitons in the quantum-well plane. E_{x1} and E_{x2} denote the energies of the 1s and 2s branches of the exciton dispersion, respectively; higher bound exciton states are omitted from this schematic representation. An electron-hole pair is excited at the continuum edge, near $\vec{K}_{\|}$, and subsequently scatters to the 1s branch.

We have selected symmetrically strained (GaIn)As/Ga(PAs) multiple quantum wells for our experiments, since the strain-induced blue-shift of the light-hole exciton allows to study the spatiotemporal evolution of the electron-heavy hole pair excitations without being disturbed by light-hole transitions. The structure was grown by metal-organic vapour phase epitaxy, and consists of 50 periods of 9.0 nm thick $InGa_{1-x}$ wells and 8.3 nm thick $GaAs_{1-y}P_y$ barriers, where x=0.11 and y=0.247 were chosen such that the strain in the structure is balanced [2,3]. Thin GaAs layers of 1.0 nm and 1.8 nm width, respectively, were grown on the two sides of each well layer to avoid quarternary interfaces. For spatial calibration purposes special gold structures with sizes between 0.5μm and 5μm were deposited on the sample surface. Fig. 2 shows an absorption spectrum of the sample at low temperature (T = 7K). The n=1 heavy-hole exciton transition and the onset of the excitonic continuum can clearly be discerned.

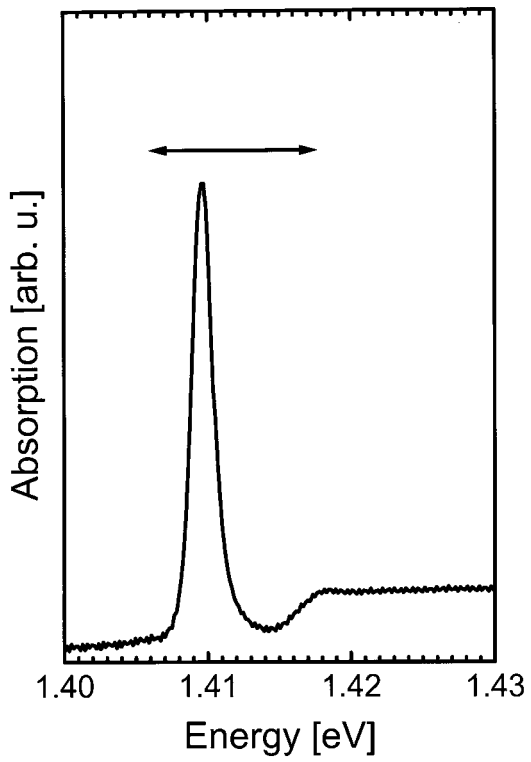

Figure 2. Absorption spectrum of the symmetrically strained (GaIn)As/Ga(PAs) multiple-quantum-well structure, at T = 7K. The horizontal bar marks the full-width-at-half-maximurm of the exciting laser pulses.

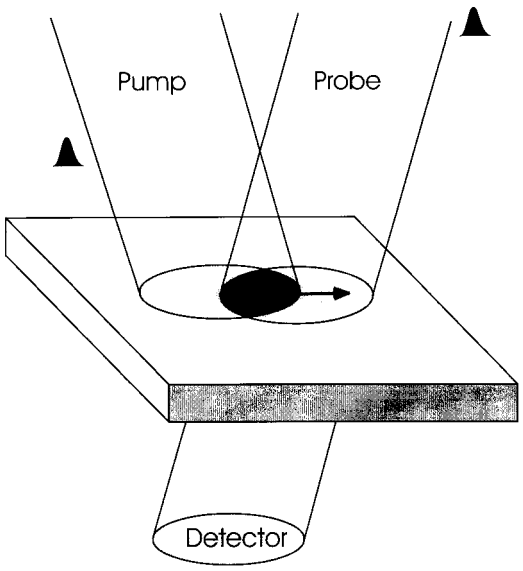

Figure 3. Principle of the spatially resolved optical pump-probe technique. Pulsed pump and probe laser beams are focussed to 1.5μm-diameter spots on the sample surface. These spots can be displaced with respect to each other with sub-μm accuracy. Carriers and excitons moving out of the overlap region of the two spots into the non-intersected region of the probe spot (as indicated by the arrow) contribute to the pump-probe signal.

For high temporal resolution we use a Kerr-lens modelocked Ti:sapphire laser providing $\approx$ 150fs pulses with a spectral width of $\approx$ 12meV. A microscope objective is used to focus pump and probe beams into a helium flow cryostat, where a spot diameter of 1.5μm is obtained on the sample surface. We limit the maximum density of optically excited e-h pairs to $2 \cdot 10^{10}\mathrm{cm}^{-2}$ to stay in the regime where the detected optical nonlinearity is proportional to the carrier density. A steering lens placed in the path of the probe beam is used to laterally displace pump and probe spots with sub-μm accuracy. The essential point about this technique is that at non-zero lateral displacements, carriers and excitons that rnove out of the overlap region of the two spots into the non-intersected region of the probe spot can contribute to the pump-probe signal (Fig. 3). It is thus possible to map out the propagation profile of e-h pairs with respect to time, by measuring pump and probe transients at different lateral displacements [4-6].

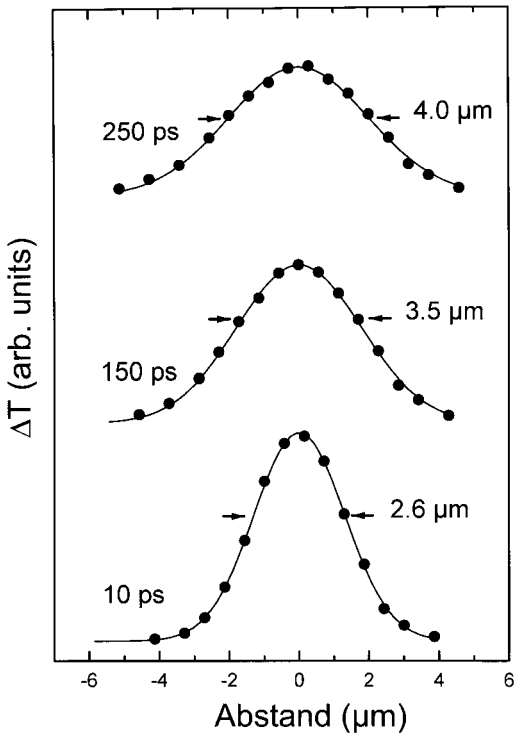

Figure 4. Plot of pump-probe signal (change in transmission ΔT) versus lateral displacement for three different time delays between pump and probe pulses.

An example is shown in Fig. 4 where the pump-probe signal (change in transmission ΔT) is plotted versus the lateral displacement for various time delays.

The width of the signal profile increases with time, due to the lateral motion of the e-h pairs [5]. Assuming Gaussian distributions for the carrier populations and the probe beam, the profiles can be nicely fitted as shown by the solid lines in Fig. 4. From the fits we deduce the spatial width Δx of the carrier population defined by the $\exp(-1/2)$-values of the respective Gaussian distribution. It can be shown for Gaussian distributions that the diffusion constant of the e-h pairs, D is given by

$$D \propto \frac{\partial}{\partial t}[\Delta x(t)]^2 \qquad (1)$$

This relation allows to deduce from the spatially resolved pump-probe measurements the diffusivity of the e-h pairs as a function of time. An example is shown in Fig. 5, where D is plotted versus time [6]. Here the sample, which is held at a temperature of 30K, is excited with pulses centered 3 meV above the heavy-hole exciton. We observe a decrease of D from $42\mathrm{cm}^2\mathrm{s}^{-1}$ to $28\mathrm{cm}^2\mathrm{s}^{-1}$. We explain this decrease with the temperature dependence of the diffusivity. The pump pulse has spectral components that extend into the excitonic continuum (cf. Fig. 2), hereby exciting free e-h pairs. Those e-h pairs will subsequently form excitons and thus gain kinetic energy (cf. Fig. 1). This process deposits a mean excess energy $E_{exc} \approx 3.6meV$ into the exciton system, resulting in an estimated exciton temperature of $T_X \approx 40K$ after thermalization. Thus T_X lies above the lattice temperature of $T_L = 30K$. Consequently the exciton distribution cools down to the lattice temperature with time, and saturates when this temperature is reached. This cooling process is observed in the time-dependent drop of the diffusivity.

In a similar way, heating of the exciton distribution can be observed. Fig. 6 shows the time dependence of D for various lattice temperatures above the initial exciton temperature of $T_X \approx 25K$. We observe an initial rise of the diffusivity, and a subsequent saturation at some value that increases with the lattice temperature. Again, the saturation indicates complete equilibration between the exciton temperature and T_L The time required for equilibration, which is given by the rise time of the transients, decreases with increased T_L This acceleration of the equilibration process can be explained by the increased scattering of free e-h pairs and excitons with phonorls when the lattice temperature is increased.

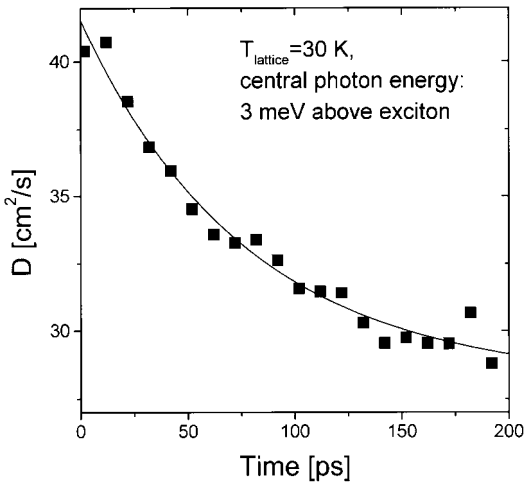

Figure 5. Plot of the diffusivity D versus delay time. The drop of D is caused by a cooling of the exciton distribution to the lattice temperature.

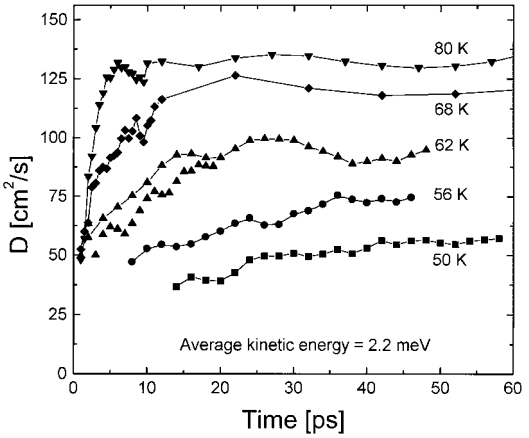

Figure 6. Plot of the diffusivity D versus delay time, at various lattice temperatures. The initial rise of D is caused by a heating of the exciton distribution to the lattice temperature.

III. Relaxation dynamics in quantum dots

In this Section, we study carrier relaxation in quantum dots (QD's) that are produced by introducing a stressor- induced lateral confinement potential in the plane of a (GaIn)As/GaAs QW. The lateral carrier localization results in relaxing the $\vec{K}_{\|}$-selection rule in the coupling to the light field so that radiative recombination should be facilitated in comparison with the QW case. Conversely, carrier scattering should be hindered in QD's insofar as the discrete density of states generated by the confinement potential can result in severe energy conservation problems. In particular, fast

LO-phonon-induced relaxation between QD levels is expected to be prohibited w henever there is a signifant mismatch between the QD level spacing and the LO-phonon energy; in those cases, phononic relaxation of carriers between QD levels can only occur via emission of acoustic phonons [8,9], which is slow. Experimentally, recent time-resolved photoluminescence (PL) measurements show that at sufficiently high carrier densities carrier relaxation is in fact very much faster than would be expected iIl the case of acoustic-phonon scattering alone [10 15]. This has been suggested to be due to fast Coulomb scattering via an Auger-like process [10-12,15] in which carriers confined in zero-dimensional QD states exchange enelgy with carriers in two-dimensional QW state,. and thus rapidly relax to lower-lying QD states [16]. To study these relaxation processes, we perform time-resolved PL experiments on (GaIn)As/GaAs QD's, as described in the following.

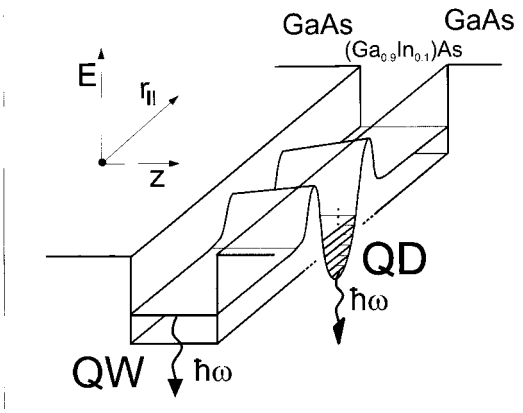

Figure 7. Schematic potential profile for electrons in the conduction band. The quantum-well (QW) potential in growth direction (z) and the strain-induced parabolic-like potential in the lateral direction ($r_{\|}$) combine to produce a wavefunction confinement in all thlee spatial directions, which gives rise to a series of quantized zero-dimensional quantum-dot (QD) levels.

The QD sample consists of a single 7 nm-thick $(Ga_{0.9}In_{0.1}As$ layer embedded within GaAs, with a GaAs top layer thickness of 5 nm. InP islands with a width of 75 nm, a height of 22 nm, and a density of approximately $2 \cdot 10^9 cm^{-2}$ were grown on this GaAs top layer via in-situ deposition of InP (Stranski-Krastanov growth mode) [17]. The InP islands act as stressors, leading to a modulation of the (GaIn)As/GaAs QW band gap in the spatial region below the InP islands. Fig. 7 shows the schematic potential profile for electrons in the conduction band. The strain-induced potential profile in the QD region has a parabolic-like shape in the lateral direction and a depth of about 70 meV with respect to the first quantized state in the QW, as shown by calculations [18]. This additional lateral confinement leads to a series of quantized QD levels as schematically drawn in Fig. 7.

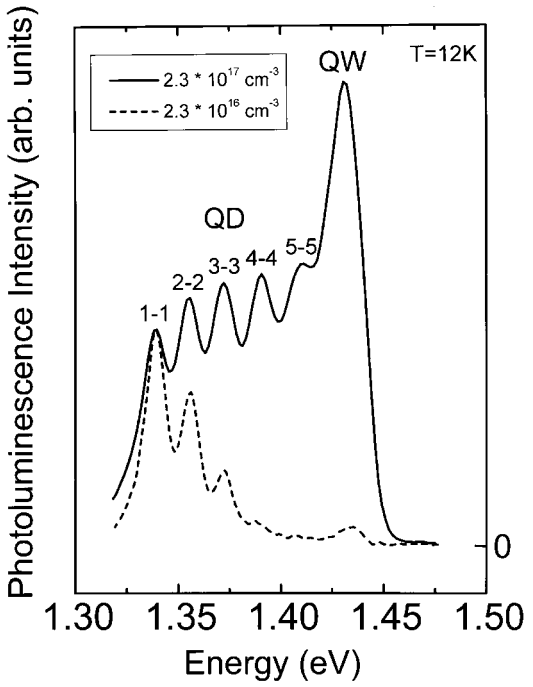

Figure 8. Low-temperature ($T = 12K$) photoluminescence spectra taken for pulsed excitation at 1.573 eV. Excitation densities are as indicated.

Fig. 8 shows low-temperature (T = 12K) PL spectra taken for pulsed excitation at a central photon energy of 1.573 eV, i.e. energetically above the GaAs band edge. Pulses with a duration of 110 fs are generated by a Kerrlens mode-locked Ti:sapphire laser, and focused onto a spot of approximately 200?m in diameter on the InP- island side of the sample. The estimated densities of carriers optically excited in the GaAs barrier region are $2.3 \cdot 10^{16} cm^{-3}$ and $2.3 \cdot 10^{17} cm^{-3}$, respectively. The PL line at about 1.43eV can be attributed to exciton recombination from the QW outside the regions covered by the InP islands. As shown by Lipsanen et al. [17] and Tulkki and Heinamaki [18], the five separate PL lines observed at lower energies in the high-density PL spectrum are due to electron-hole recombination between QD states of the conduction- and valence-band. Calculations show that the conservation rule $\Delta i = 0$ holds to a good approximation for the 'interband' QD transitions [18], where i = 1,2,3... labels the QD states

(from lower to higher energies); accordingly we have labeled the QD transitions as $i-i$. The spectrum taken at low excitation density shows a strong PL signal from the 1-1 transition. It is only at higher excitation densities that the higher-lying transitions, including the QW transition, give a larger contribution to the PL since then state filling in the QD states becomes sufficiently significant as to impede carrier relaxation (Pauli blocking) [17].

The time-resolved PL experiment is performed under the same excitation conditions as in the measurement of the temporally integrated spectra shown in Fig. 8. Time resolution is obtained by mixing the PL from the sample with a delayable reference laser pulse (which has the same photon energy as the excitation pulse) in a nonlinear BBO crystal to generate a sum-frequency signal [1]. The up-converted signal is dispersed by a monochromator with a spectral resolution of 2 meV, and is detected by a cooled photomultiplier. The temporal resolution of the set-up is approximately 220 fs. Due to the small temporal overlap of the 110 fs reference pulse with the long-lasting (some ns) QD PL, special care has to be taken to optimize the signal-to-noise ratio of the experiment.

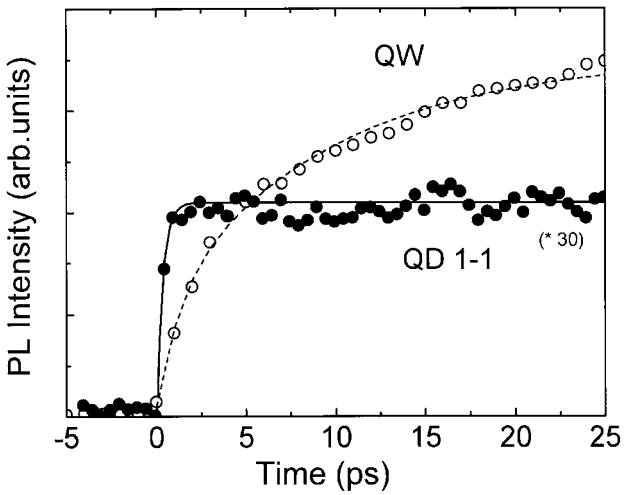

Figure 9. Photoluminescence transients taken at the spectral position of the quantum-dot 1-1 and the quantum-well transitions (T = 12K).

Fig. 9 shows PL transients taken at the spectral positions of the QD 1-1 transition (closed circles) and the QW transition (open circles), respectively (at an excitation density of $7.0 \cdot 10^{16}\mathrm{cm}^{-3}$ in the GaAs barrier region). The QD 1-1 PL shows an extremely rapid initial rise before reaching a constant intensity [19]. In contrast, the QW PL shows a much slower rise. This difference is particularly striking in view of the fact that the photoexcited carriers need to relax more energy to be captured into the QD states than into the QW states, since the QD states are considerably lower in energy (cf. Figs. 7 and 8). This difference in the PL rise rates can be explained in the following way. The QW PL originates from excitons that have relaxed to states of vanishing in-plane center-of-mass momentum ($K_{\|} \approx 0$), where radiative recombination can occur. It is well known that for nonresonant excitation this long rise time is due to cooling of the hot exciton distribution in the QW [20,21]. In contrast, the lateral carrier localization in the QD results in a breakdown of the ($K_{\|}$-selection rule in the radiative recombination process [7]. Accordingly, the cooling of the hot e-h distribution within the QD potential does not lead to a long-lasting QD-PL onset. We note that this is useful for the measurement of the relaxation dynamics in the QD's. In contrast to Section I of this paper, where a rather sophisticated experimental technique had to be used to gain access to the e-h pair dynamics away from ($K_{\|} \approx 0$), in the QW, in QD's the relaxation dynamics of the entire e-h distribution is directly accessible by optical means.

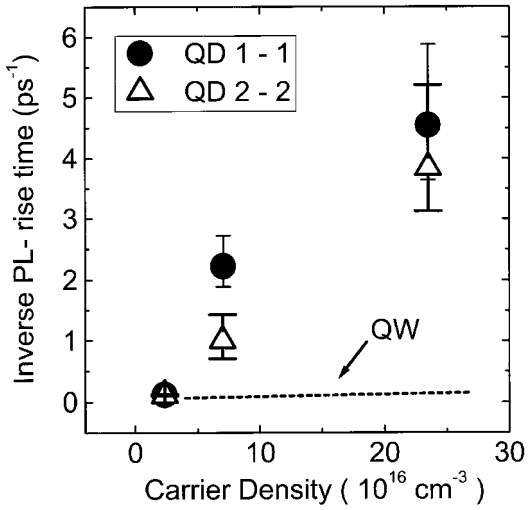

Figure 10. Inverse photoluminescence rise time τ_{rise}^{-1} versus excitation density in the embedding GaAs material for the 1-1 (filled circles) and 2-2 (triangles) quantum-dot transitions. The error bars indicate the uncertainties in the fits to the quantum-dot luminescence transients. The dashed line indicates the inverse rise times found for the exitonic (GaIn)As/GaAs quantum-well luminescence.

As a consequence of the aforesaid, the PL rise time in the QD, τ_{rise} is expected to give a good measure of the carrier capture time into the QD states. We fit

the PL transients with a function of the form $I(t) = I_0(1-\exp(-t/\tau_{rise}))$, and obtain $\tau_{rise} = 0.45ps$ for the 1-1 transient in Fig. 7. This shows that carrier capture into the QD ground state occurs on a subpicosecond time scale at this excitation density. The capture times are density-dependent, as shown in Fig. 10, where we have plotted the inverse PL rise times τ_{rise}^{-1} extracted from the 1-1 PL transients versus the excitation density (filled circles). The corresponding values of τ_{rise}^{-1} for the 2-2 PL are also plotted (hollow triangles). In both cases the PL rise rate, and hence the capture rate, increases with increased excitation density. A similar density dependence is theoretically expected for Auger-like relaxation of QD carriers via Coulomb scattering with carriers in 2D and 3D states [16]. It is therefore reasonable to assume that it is this mechanism which governs the relaxation into the lower QD states in our experimelIt [22]. This is further confirmed by the extremely large absolute values of τ_{rise}^{-1} at high excitation densities (in particular at $2.3 \cdot 10^{17}\mathrm{cm}^{-3}$), which are incompatible with relaxation due to electron-phonon scattering. These results, which have been obtained with the high time resolution of the present experiment, thus corroborate interpretations of earlier PL experiments that have invoked fast Coulomb scattering to explain the temporal profile of QD-PL transients [10-12,15].

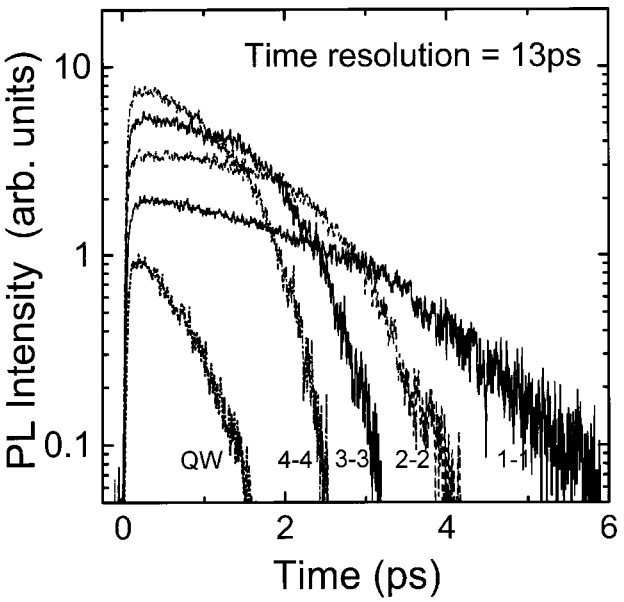

Figure 11. Photoluminescence transients taken at the spectral positions of the four lowest quantum-dot transitions and the (GaIn)As/GaAs quantum-well exciton transition, on a ns-time scale. The quantum-well luminescence intensity is scaled down by a factor of 100 with respect to the quantum-dot luminescence intensities.

So far we have studied the rise of the QD-PL transients. In the following, we will analyze their temporal decay, to extract information on recombination lifetimes and phonon-mediated inter-level scattering times. To record the PL transients over large time intervals, we use a streak camera system providing a temporal resolution of about 13 ps. In Fig. 11 the results of time- resolved PL measurements taken under the same excitation conditions as in Fig. 9 are shown for the QW PL and the four lowest QD transitions (1-1, 2-2, 3-3, and 4- 4) in a semilogarithmic plot. After the signal rise (which seems slower than in Fig. 9 due to the more limited time resolution of the streak camera system) the QD PL transients show plateaulike temporal profiles before they successively start to decay after 1.5 - 3.5 ns. The relative intensities of the various QD PL transients scale nicely with the respective values of the calculated degeneracies $D_i = 2i$. This experimental result means that the lower QD levels are almost fully occupied at the maxima of the PL transients. These occupations will remain essentially constant as long as carlier feeding from energetically higher states balances any losses caused by recombination or relaxation into lower states. Changes of slope in the PL transients appear when the occupation begins to drop as a consequence of any decrease in the feeding rate. The sequence of decays in Fig. 11 thus reflects the drop of the quasi-Fermi level in the QD with time.

After about 4 ns there is only the PL from the lowest QD transition (1-1) left. Since at these late times feeding processes from higher states have completely ceased, the 1-1 PL decays exponentially. We thus identify its decay time of $860 \pm 25ps$ with the pure recombination lifetime τ_{rec} of the lowest QD transition. Due to the facts that (i) the QD is just a strained region of a high-quality QW with no contaminated interfaces, (ii) the QD PL has an extremely high efficiency, (iii) the decay time of the QD is longer than that of the QW, we assume that $\tau_{rec} = 860ps$ is the optical lifetime. This assignment is further confirmed by measuring the temperature dependence of the PL decay rate. which is found to be independent of temperature up to about 80 K. The PL decays of the higher-energetic QD transitions are faster than that of the 1-1 transition. As shown by model calculations described in more detail elsewhere [15], this is due to inter-level relaxation me-

diated by OD-2D Coulomb scattering (as long as carriers are present in the QW) and by acoustic phonon scattering. These model calculations are based on the assumptions that the OD-2D scattering rate is proportional to the 2D carrier density in the QW, and that carriers can only relax to lower-lying *non-occupied* QD states. The calculations yield good fits to the experimental PL transients for an acoustic phonon scattering time of $\tau_{ph} = 570ps$. The fitted value for the interlevel relaxation time induced by Coulomb scattering is $\approx$ 1ps right after the optical excitation, and is hence of the same order of magnitude as the capture time determined from the rise of the 1-1 transient in Fig. 9.

IV. Summary

In the first part of the present article, we have shown that it is possible to study the dynamics of QW e-h pairs with non-zero in-plane wavevector ($\vec{K}_{\|} \neq 0$) by making use of the fact that the momentum distribution of those e-h pairs is reflected in their spatial motion. We have performed temporally and spatially resolved optical pump-probe experiments on strained (GaIn)As/Ga(PAs) QW's. In this way, the lateral diffusivity of excitons as a function of time and crystal temperature has been studied. The results of these measuremeIIts clearly show the cooling and heating dynamics of the exciton distribution spread in ($\vec{K}_{\|}$-space. In the second part of the present article, we have studied carrier relaxation in QD's that are produced by introducing a stressor-induced lateral confinement potential in the plane of a (GaIn)As/GaAs QW. The localization-induced breakdown of the $\vec{K}$-selection rule in the radiative recombination process allows to optically monitor the relaxation dynamics of the entire e-h distribution in the QD's. We have performed time- resolved PL experiments on the QD structure. We observe a sub-picosecond onset of the QD PL, with a density dependence that is consistent with carrier relaxation via Coulomb scattering. This relaxation process is important as long as there is a sufflcient density of carriers in higher-dimensional states. From the decay of the transients, we have extracted the optical lifetime of carriers in the QD, and the time constant for acoustic-phonon-induced scattering of electrons between QD levels.

Acknowledgements

We thank R. Arnold, S. Grosse, J.H.H. Sandmann, and G. Hayes for performing the time-resolved measuIements reported in this article. The photoluminescence up- conversion experiments were performed in the laboratories of R. Philipps at the University of Cambridge, whom we also thank for useful discussions. We thank A. Kriele and J.P. Kotthaus for depositing the calibration gold masks on the (GaIn)As/Ga(PAs) multiple- quantum-well sample, and M. Koch and M. Perner for linear absorption measurements. Helpful discussions with J. Tulkki, M. Brasken, and W. Spirkl are gratefully acknowledged. Specia.l thanks are due to R. Rettig, T. Marschner, and W. Stolz for supplying the (GaIn)As/Ga(PAs) multiple- quantum-well structure, and to H. Lipsanen, M. Sopanen, and J. Ahopelto for the high-quality (GaIn)As/GaAs quantum-dot structure. The work has been financially supported by the Deutsche Forschungsgemeinschaft (Grant No. Fe 323/5- 1 and Fe 323/3-2) and by the European Union (Network Ultrafast Processes in Semiconductors).

References

1. see e.g., J. Shah, *Ultrafast Spectroscopy of Semiconductors and Semiconductor Nanostructures* (Springer, Berlin, 1996).
2. S. Lutgen, T.F. Albrecht, T. Marschner, W. Stolz and E.O. Gobel, Solid-State Electronics **37**, 905 (1994).
3. S. Lutgen, T. Marschner, W. Stolz, E.O. Gobel and L. Tapfer, J. Crystal Growth **152**, 1 (1995).
4. H.W. Yoon, D.R. Wake, J.P. Wolfe and H. Morko, Phys. Rev. B **46**, 13461 (1992).
5. S. Grosse, R. Arnold, A. Kriele, G. von Plessen, J.P. Kotthaus, J. Feldmann, R. Rettig, T. Marschner and W. Stolz, in *Spring Topical Meeting on 'Quantum Opto- electronics'*, Hyatt Lake Tahoe (Nevada USA, 1997).
6. R. Arnold, S. Grosse, A. Kriele, G. von Plessen, J.P. Kotthaus, J. Feldmann, R. Rettig, T. Marschner and W. Stolz (to be published).
7. R. Cingolani, Y.H. Zhang, R. Rinaldi, M. Ferrara and K. Ploog, Surface Science **267**, 457 (1992).

8. U. Bockelmann and G. Bastard, Phys. Rev. B **42**, 8947 (1990) .
9. T. Inoshita and H. Sakaki, Solid-State Electronics **37**, 1175 (1994).
10. J.H.H. Sandmann, S. Grosse, J. Feldmann, H. Lipsanen, M. Sopanen, J. Tulkki and J. Ahopelto, Nuov. Cim. D **17**, 1699 (1995).
11. U. Bockelmann, P. Roussignol, A. Filoramo, W. Heller, G. Abstreiter, K. Brunner, G. Bhm, and G. Weirma Phys. Rev. Lett. **76**, 3622 (1996).
12. F. Adler, M. Geiger, A. Bauknecht, F. Scholz, H. Schweizer, M.H. Pilkuhn, B. Ohnesorge and A. Forchel, J. Appl. Phys. **80**, 4019 (1996).
13. M. Vollmer, E..J. Mayer, W.W. Rhle, A. Kurtenbach and K. Eberl, Phys. Rev. B **54**, 17292 (1996).
14. S. Raymond, S. Fafard, P.J. Poole, A. Wojs, P. Hawrylak, S. Charbonneau, D. Leonard, R. Leon, P.M. Petroff, and J.L. Merz, Phys. Rev. B **54**, 11548 (1996).
15. S. Grosse, J.H.H. Sandmann, G. von Plessen, J. Feldmann, H. Lipsanen, M. Sopanen, J. Tulkki and J. Ahopelto, Phys. Rev. B **55**, 4473 (1997).
16. U. Bockelmann and T. Egeler, Phys. Rev. B**46**, 15574 (1992) .
17. H. Lipsanen, M. Sopanen and J. Ahopelto, Phys. Rev. B**51**, 13868 (1995).
18. J. Tulkki and A. Heinamaki, Phys. Rev. B**52**, 8239 (1995).
19. J.H.H. Sandmann, G. von Plessen, J. Feldmann, G. Hayes, R. Phillips, H. Lipsanen, M. Sopanen and .J. Ahopelto (to be published).
20. P.W.M. Blom, P.J. van Hall, C. Smit, J.P. Cuypers and J.H. Wolter, Phys. Rev. Lett. **67**, 2335 (1991).
21. Y. Rosenwaks, M.C. Hann, D.H. Levi, D.M. Szrnycl, R.K. Ahrenkiel and A.J. Nozik, Phys. Rev. B **48**, 14675 (1993) .
22. At very low excitation densities, the number of carriers being directly captured into the QD is insuffient to fill the QD completely so that carrier transport prior to capture slows down the PL rise; this leads to some additional density dependence of the PL rise rate at very low densities.